Vacuum Ultraviolet Circular Dichroism Studies of Simple Saccharides

Edward R. Arndt and Eugene S. Stevens*

Contribution from the Department of Chemistry, State University of New York, Binghamton, New York 13902-6000

Received March 1, 1993

Abstract: The circular dichroism (CD) of simple sugars was extended to 140 nm using film samples. The 150–190-nm region can be decomposed into four components. The signs of these four components are strictly correlated with anomeric configuration. Dominant contributions to CD arise from electronic transitions localized on the oxygen atoms of the ether chromophores. The CD below 150 nm represents the onset of the lowest energy σ–σ^* transition, the sign of which is also correlated with anomeric configuration. By extrapolation, its center is estimated to be at approximately 120–130 nm. The CD spectra of representative disaccharides contain a conformation-dependent contribution, indicating the usefulness of CD as a conformational probe. The results reported here provide a basis for developing improved interpretive models.

The planetary biomass is overwhelmingly dominated by carbohydrate, largely because of the abundance in the plant world of two polymers of D-glucose (cellulose and starch),[1] and the increased commercial use of carbohydrate materials has been accompanied by greater attention to their chemical and physicochemical properties.[2] Characterization at the molecular level has progressed through the application of many techniques in conjunction with one another.[3]

Chiroptical properties are very sensitive to chemical structure, configuration, and conformation.[4] This sensitivity places great demands on models aimed at allowing the interpretation of chiroptical properties in terms of conformation. Any interpretive model must relate not only correctly but also in detailed fashion the dependence of chiroptical properties on the geometric arrangement of atoms. Furthermore, unsubstituted saccharides absorb only below 190 nm; the electronic transitions responsible for their chiroptical properties are, therefore, not readily accessible. To date, only the weak CD band near 183 nm has been characterized,[5] and an empirically derived sector rule has been proposed for the 175-nm CD band observed in polysaccharides.[6] The observed vacuum ultraviolet CD (VUCD) of aqueous saccharide solutions[7] and of polysaccharide films[8] is generally too weak to account for the measured Na_D optical rotation, demonstrating the important role of even higher energy electronic transitions. Observed Na_D rotations can be reproduced with a calculational model which attributes the rotation to the coupling of high energy, bond localized σ–σ^* transitions, but the model is highly parametrized.[9,10]

The purpose of the present study was to provide a more detailed characterization of the electronic transitions in simple saccharides so as to allow the further development of interpretive models for the conformation dependence of their chiroptical properties.

Experimental Methods

Seven monosaccharides and five disaccharides were examined.[11] All samples, with the exception of xylobioside, were obtained from Pfanstiehl Laboratories, Inc., Waukegan, IL, and used without further purification. Xylobioside was provided by Dr. S. Bystricky, Institute of Chemistry, Slovak Academy of Sciences, Bratislava, Czechoslovakia.

Films were prepared from "Gold label" 2,2,2-trifluoroethanol (Aldrich Chemical Co., Milwaukee, WI) solutions (4 mg/mL or at saturation). Five to twenty drops of solution were placed on a level 1-cm diameter CaF_2 window. The pressure was slowly reduced until a clear interference rainbow became evident and then further reduced to approximately 1 Torr for 10–15 min, assuring sufficient film setting to prevent humidity damage during later transfer to the spectrometer. While most films prepared in this manner were air stable for at least 10 min, some required dry conditions at all times. The key requirement for satisfactory films appeared to be maintaining a vacuum level such that evaporation of the supersaturated solution was fast enough to avoid crystallization, and subsequent birefrigence, yet slow enough to avoid vapor bubble formation which leads to film breakup.

For some samples, it was necessary to place a second window against the film to eliminate sample loss through evaporation in the vacuum monochromator. In these cases, lower light throughput required a reduced film thickness.

(1) Lehninger, A. L. *Biochemistry*; Worth: New York, 1975.
(2) *Industrial Polysaccharides: The Impact of Biotechnology and Advanced Technologies*; Stivala, S. S., Crescenzi, V., Dea, I. C. M., Eds.; Gordon and Breach: New York, 1987.
(3) (a) *Solution Properties of Polysaccharides*; ACS Symp. Ser. 150; Brant, D. A., Ed.; American Chemical Society: Washington, DC, 1981. (b) *Polysaccharides: Topics in Structure and Morphology*; Atkins, E. D. T., Ed.; VCH: Deerfield Beach, FL, 1985. (c) *Biopolymers*; Adv. Polym. Sci., No. 83; Springer-Verlag: New York, 1987.
(4) Morris, E. R.; Frangou, S. A. In *Techniques in Carbohydrate Metabolism*; Elsevier: London, 1981; B308, pp 109–160.
(5) (a) Listowsky, I.; Englard, S. *Biochem. Biophys. Res. Commun.* **1968**, *30*, 329–332. (b) Johnson, W. C., Jr. *Adv. Carbohydr. Chem. Biochem.* **1987**, *45*, 73–124. (c) Texter, J.; Stevens, E. S. *J. Chem. Phys.* **1979**, *70*, 1440–1449.
(6) Cziner, D. G.; Stevens, E. S.; Morris, E. R.; Rees, D. A. *J. Am. Chem. Soc.* **1986**, *108*, 3790–3795.
(7) (a) Nelson, R. G.; Johnson, W. C., Jr. *J. Am. Chem. Soc.* **1976**, *98*, 4296–4301. (b) Lewis, D. G.; Johnson, W. C., Jr. *Biopolymers*, **1978**, *17*, 1439–1449.
(8) (a) Stevens, E. S.; Morris, E. R. *Carbohydr. Polym.* **1990**, *12*, 219–224. (b) Duda, C. A.; Stevens, E. S.; Reid, J. S. G. *Macromolecules* **1991**, *24*, 431–435.
(9) (a) Stevens, E. S.; Sathyanarayana, B. K. *Carbohydr. Res.* **1987**, *166*, 181–193. (b) Stevens, E. S.; Sathyanarayana, B. K. *Biopolymers* **1988**, *27*, 415–421. (c) Stevens, E. S.; Sathyanarayana, B. K. *J. Am. Chem. Soc.* **1989**, *111*, 4149–4154.
(10) (a) Duda, C. A.; Stevens, E. S. *J. Am. Chem. Soc.* **1990**, *112*, 7406. (b) Duda, C. A.; Stevens, E. S. *Carbohydr. Res.* **1990**, *206*, 347–351. (c) Stevens, E. S.; Duda, C. A. *J. Am. Chem. Soc.* **1991**, *113*, 8622–8627. (d) Duda, C. A.; Stevens, E. S. *Biopolymers* **1991**, *31*, 1379–1385. (e) Duda, C. A.; Stevens, E. S. *Carbohydr. Res.* **1992**, *228*, 333–338.
(11) The disaccharides were trehalose [1-1-O-α-D-glucopyranosyl-α-D-glucopyranoside], cellobiose [1-4-O-β-D-glucopyranosyl-D-glucopyranose], lactose [1-4-O-β-D-galactopyranosyl-D-glucopyranose], melibiose [1-6-O-α-D-galactopyranosyl-D-glucopyranose], and xylobioside [methyl 1-4-O-β-D-xylopyranosyl-β-D-xylopyranoside].

0002-7863/93/1515-7849$04.00/0 © 1993 American Chemical Society

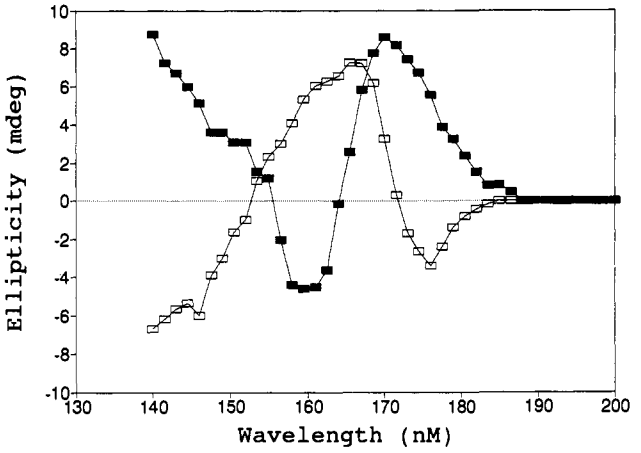

Figure 1. VUCD of methyl α-D-glucopyranoside (■) and methyl β-D-glucopyranoside (□).

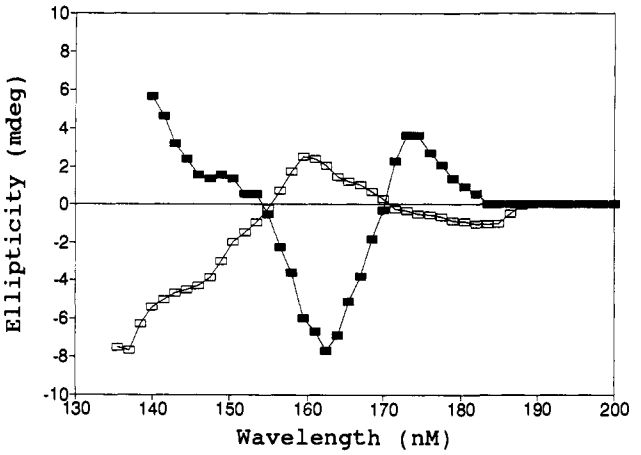

Figure 2. VUCD of methyl α-D-xylopyranoside (■) and methyl β-D-xylopyranoside (□).

The VUCD spectrometer has been previously described in detail.[12] It was used with a deuterium light source, a spectral resolution of 3.2 nm, a scan rate of 1.0 nm/min, and a time constant of 100 s. Calibration was carried out with (+)-10-camphorsulfonic acid, and results reported in units of ellipticity, θ, with an estimated uncertainty of ±1 mdeg. Spectra were digitized using visual averaging over a 3-nm interval; three to five spectra were averaged to produce the reported spectra.

Cellobiose, lactose, and melibiose samples were present in solution as an equilibrium mixture of both anomeric forms of the reducing residue, D-glucose, which, however, was not a major limitation for the present purposes of determining the number and location of CD components.

Results

CD spectra of the seven methyl pyranosides are shown in Figures 1–4. Although there are usually two CD extrema above 150 nm, the band shapes strongly suggest the presence of more than two overlapping CD components, e.g., a shoulder often appears near 183 nm on the next higher energy CD band, and the widths of the CD bands between 150 and 180 nm vary from 6 to 13 nm. Comparison of the seven monomer spectra suggests a total of four bands in the 150–190-nm range. In some cases an additional, weak CD feature appears near 148 nm, but because of the increasing CD intensity at shorter wavelengths in most spectra, further interpretation of it was not attempted. The occasional sign differences between the film CD and the solution CD spectra reported by Nelson and Johnson[7a] are likely the result of the conformational flexibility of exocyclic groups.

(12) Pysh (Stevens), E. S. *Annu. Rev. Biophys. Bioeng.* **1976**, *5*, 63–75.

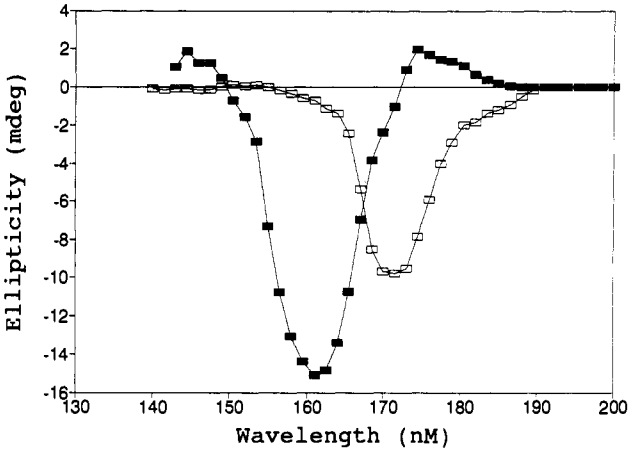

Figure 3. VUCD of methyl α-D-galactopyranoside (■) and methyl β-D-galactopyranoside (□).

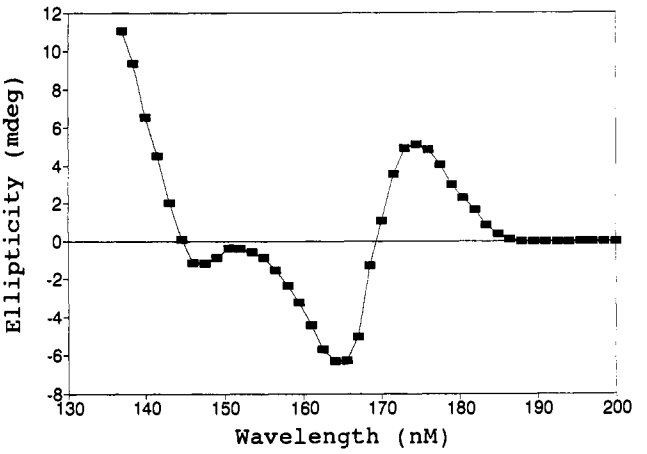

Figure 4. VUCD of methyl α-D-mannopyranoside.

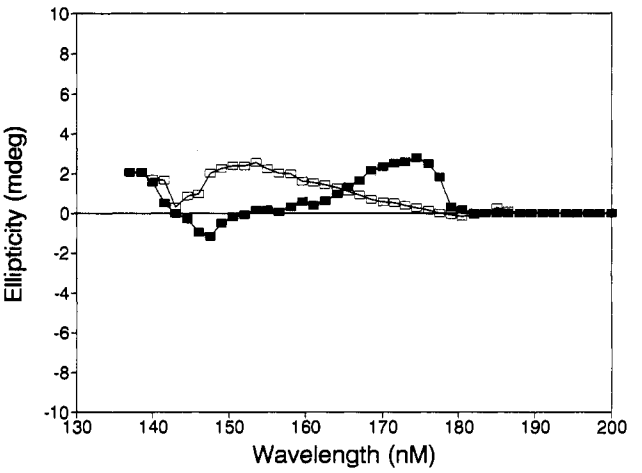

Figure 5. VUCD of trehalose (■) and cellobiose (□).

The disaccharide CD spectra (Figures 5 and 6) have features qualitatively resembling those of the monomer components, but they are clearly not additive combinations. The dominance of the positive 170-nm CD component in α-D-glucopyranoside is evident in the spectrum of trehalose. The broad positive CD from 152 to 170 nm in β-D-glucopyranoside is also found in the spectrum of cellobiose. The 162- and 175-nm components of the β-D-xylopyranoside spectrum appear in the xylobioside spectrum, but with sign inversion. The broad negative CD in β-D-galactopyranoside from 150 to 190 nm also characterizes the CD of lactose. The CD of melibiose seems to be the least related to the CD of its monomer components. A conformation-dependent

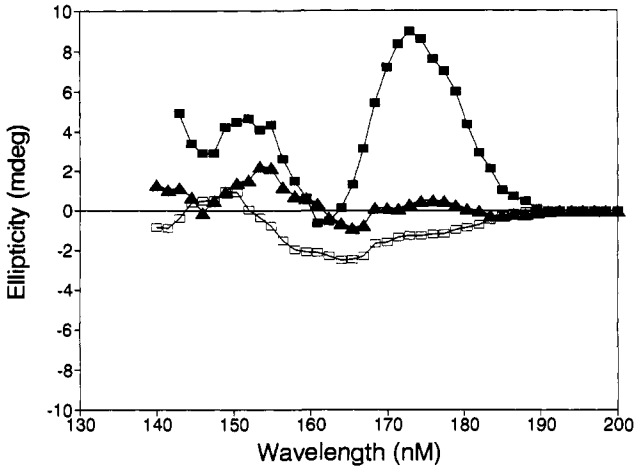

Figure 6. VUCD of lactose (□), melibiose (■), and xylobioside (▲).

component in the CD of maltose has been reported by Lewis and Johnson.[7b]

Discussion

150–190-nm CD. As noted previously, the spectral features for the monomers suggest four bands above 150 nm. The CD spectra from 150 to 190 nm were therefore deconvoluted into four Gaussian components (eq 1).

$$\theta = \sum_i \theta_i^\circ \exp[-(\lambda - \lambda_i^\circ)^2/(\Delta\lambda_i)^2] \qquad (1)$$

By inspection, fitting commenced with the bands initially centered at 160, 168, 174, and 183 nm and with an initial uniform bandwidth of 6 nm. Optimization was constrained to yield a common set of four band centers and four bandwidths for the seven methyl pyranosides. The fitted curves represent all points in the seven spectra to within experimental error. So as to display the experimental uncertainty explicitly, the θ_i° were not scaled to constant film thickness; the four band centers and widths were unaffected. Isolation of the data above 150 nm was aided by the appearance of a CD crossover in sign near 150 nm in all monomer spectra.

The results of the deconvolution are shown in Table I. There is a strict correlation between the sign of the CD and the anomeric configuration for all four CD components to within the experimental uncertainty: the 183- and 171-nm components are positive in α-pyranosides and negative in β-pyranosides; the 168- and 160-nm components are negative in α-pyranosides and positive in β-pyranosides. The strict anomeric dependence found in the present work is not observed in solution.[7a]

The lowest energy electronic transition in saturated oxocompounds has previously been assigned[5c,13] to $n_0(2p) \rightarrow \sigma^*/3s$, where the originating orbital is a nonbonding oxygen-centered lone-pair orbital, and the terminating orbital is an admixture of the lowest lying σ^* valence orbital and the oxygen 3s Rydberg orbital. In pyranosides, the transition is localized on the ether oxygen atoms.[5b] As a first approximation, we take the two ether groups of the acetal to be independent. The local point group is then C_{2v}; the transition becomes optically active through the disymmetric field of the rest of the molecule. Orbital and state designations are shown in Table II.[14] The 183-nm transition ($A_1 \rightarrow B_1$) is both electric dipole (μ_x) and magnetic-dipole (m_y) allowed.

Earlier model calculations[5c] indicated that the dominant CD mechanism for the 183-nm band is the μ–**m** variant of dynamic coupling,[18] in which the CD intensity is proportional to $-\sum V_j \mu_j \cdot \mathbf{m}$ where **m** is the magnetic-dipole transition moment of the chromophore, and μ_j are electric-dipole transition moments localized on the remaining groups of the molecule. The coupling potential, V_j, is dominated by the dipole–dipole term in the interaction between the chromophoric transition moment, μ, and the μ_j. For the μ–**m** coupling mechanism there is in general no CD symmetry rule,[18] but the two symmetry planes in C_{2v} suggest that a quadrant rule may be operative, given the dominance of the dipole–dipole term in V_j.

The likelihood that the next higher energy transitions terminate in oxygen 3p Rydberg orbitals has been discussed previously,[5c,13] and the present data support that picture; CD is often informative about symmetry species when molecular geometry is known. The 3p manifold, split by the field of the molecule, yields three transitions: $A_1 \rightarrow B_1$ ($3p_z$), $A_1 \rightarrow A_2$ ($3p_y$), and $A_1 \rightarrow A_1$ ($3p_x$). Evidence that the 171-nm CD band reflects the $A_1 \rightarrow B_1$ transition to $3p_z$ comes from the similar sign of CD for the 183- and 171-nm bands throughout the pyranoside series (Table I) and the lack of alternative orbitals of appropriate symmetry (Table II). The 168- and 160-nm CD bands are also uniformly of the same sign, within experimental error (Table I). The $A_1 \rightarrow A_2$ ($2p_x \rightarrow 3p_y$) Rydberg transition and the $A_1 \rightarrow A_2$ ($2p_x \rightarrow \sigma^{*\prime}$) valence transition are magnetic-dipole allowed (Table II) and are thereby more likely responsible for the CD than the magnetic-dipole forbidden $A_1 \rightarrow A_1$ transitions. The 168- and 171-nm CD bands have similar bandwidths (Table I), and on that basis we tentatively assign the 168-nm band to the Rydberg transition.

For the 171-nm $A_1 \rightarrow B_1$ ($3p_z$) transition, an empirical quadrant rule has been proposed which rationalizes the observed CD sign in a large number of polysaccharides.[6] The empirical quadrant rule may simply reflect the similarity in the symmetries of the two lowest energy transitions and a similarity in the coupling energetics. The Rydberg transition, however, will have a significant quadrupole component, and in addition, the $3p_z$ orbital has a nodal plane perpendicular to the two symmetry planes. These factors may give rise to an octant rule which is not revealed in polysaccharide spectra. Detailed model calculations may clarify this matter.

Similarly, the 168- and 160-nm transitions also comprise a Rydberg-valence pair, but of $A_1 \rightarrow A_2$ symmetry, that may prove to be characterized by symmetry rules in close correspondence to those of the two low-energy transitions.

The foregoing analysis is summarized in the orbital energy level diagram shown in Figure 7. The present results provide the experimental data needed to guide the development of detailed calculational models for saccharide CD in the 150–190-nm region. The fact that the disaccharide spectra (Figures 5 and 6) are clearly not additive combinations of monomer component spectra demonstrates that the CD in the 150–190-nm region depends on conformation as well as configuration, making the development of such calculational models worthwhile.

CD below 150 nm. We assign the CD below 150 nm to the onset of the lowest energy valence σ–σ^* transition. It is this transition that has been described as being responsible for the Na_D rotation of simple sugars; the lower-energy CD is too weak to account for the observed rotations.[9,10]

In order to place bounds on the band center of the σ–σ^* transition, we have fit the rising portion of the CD at 140–150 nm in the methyl α-D-glucopyranoside spectrum with two limiting

(13) Robin, M. B. *Higher Excited States of Polyatomic Molecules*, Academic Press: New York, 1974; Vol. I.

(14) C_{2v} is unique in having two σ_v symmetry planes and convention on labeling symmetry species has varied. Thus, the 2p oxygen centered orbital, antisymmetric with respect to the molecular plane, has been denoted $2p_x[b_1]$,[15] $2p_y[b_2]$,[16] and $2p_x[b_2]$.[17] We follow Mulliken and Herzberg.

(15) (a) Mullikin, R. S. *J. Chem. Phys.* **1935**, *3*, 506–514. (b) Herzberg, G. Molecular Spectra and Molecular Structure. *Electronic Spectra and Electronic Structure of Polyatomic Molecules*; van Nostrand: Princeton, NJ, 1966; Vol. II.

(16) Eyring, H.; Walter, J.; Kimball, G. E. *Quantum Chemistry*; Wiley: New York, 1944.

(17) Snyder, L. C.; Basch, H. *Molecular Wave Functions and Properties*; Wiley: New York, 1972.

(18) Schellman, J. A. *Acc. Chem. Res.* **1968**, *1*, 144–151.

Table I. Deconvolution of Methyl Pyranoside CD Spectra (Eq 1)

compound	θ° (mdeg) λ° = 160 nm $\Delta\lambda$ = 5.4 nm	λ° = 168 nm $\Delta\lambda$ = 6.1 nm	λ° = 171 nm $\Delta\lambda$ = 6.4 nm	λ° = 183 nm $\Delta\lambda$ = 4.9 nm
methyl α-D-glucopyranoside	-4.5	-1.6	10.2	1.1
methyl β-D-glucopyranoside	3.6	14.8	-11.2	-0.1
methyl α-D-xylopyranoside	-4.5	-11.9	11.4	-0.1
methyl β-D-xylopyranoside	1.7	1.9	-1.7	-1.0
methyl α-D-galactopyranoside	-14.4	-9.6	7.3	0.4
methyl β-D-galactopyranoside	-0.3	5.3	-14.0	-1.2
methyl α-D-mannopyranoside	-2.1	-17.0	16.7	0.7

Table II. Orbital and State Assignments for Low-Lying CD Bands in Simple Sugars

λ, nm	orbital designation	state designation	allowed transition dipoles[a]
183	$n_0(2p_x)[b_1] \rightarrow \sigma^*/3s[a_1]$	$A_1 \rightarrow B_1$	μ_x, m_y
171	$n_0(2p_x)[b_1] \rightarrow 3p_z[a_1]$	$A_1 \rightarrow B_1$	μ_x, m_y
168	$n_0(2p_x)[b_1] \rightarrow 3p_y[b_2]$	$A_1 \rightarrow A_2$	m_z
160	$n_0(2p_x)[b_1] \rightarrow \sigma^{*\prime}[b_2]^b$	$A_1 \rightarrow A_2$	m_z
	$n_0(2p_x)[b_1] \rightarrow 3p_x[b_1]$	$A_1 \rightarrow A_1$	μ_z
	$n_1(2p_x)[a_1] \rightarrow \sigma^*/3s[a_1]$	$A_1 \rightarrow A_1$	μ_z
120–130	$\sigma[b_2] \rightarrow \sigma^*/3s[a_1]$	$A_1 \rightarrow B_2$	μ_y, m_x

[a] μ, electric transition dipole; $\mathbf{m}$, magnetic transition dipole. [b] $\sigma^{*\prime}$ is the antisymmetric combination of the two O–C bond orbitals.

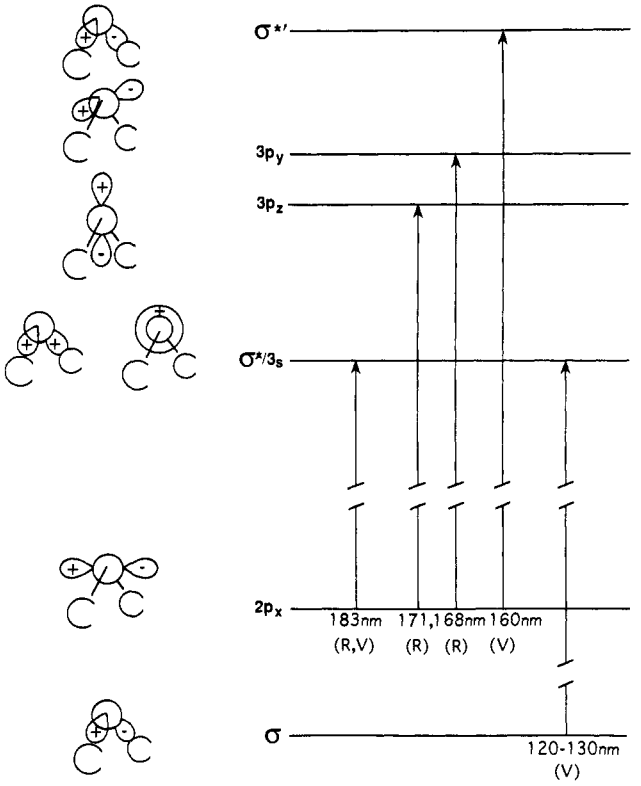

Figure 7. Orbital energy level diagram for the VUCD of simple sugars.

band shape assumptions,[19] Lorentzian (eq 2) and Gaussian (eq 3).

$$[\theta] = [\theta^\circ](\Delta\lambda)^2/[(\lambda - \lambda^\circ)^2 + (\Delta\lambda)^2] \quad (2)$$

$$[\theta] = [\theta^\circ] \exp[-(\lambda - \lambda^\circ)^2/(\Delta\lambda)^2] \quad (3)$$

In each case the band center (λ°) and bandwidth ($\Delta\lambda$) were fit to the data points, while $[\theta^\circ]$ was determined mainly by the observed Na_D rotation compared with the calculated value from

(19) Condon, E. U. *Rev. Mod. Phys.* **1937**, *9*, 432–457.

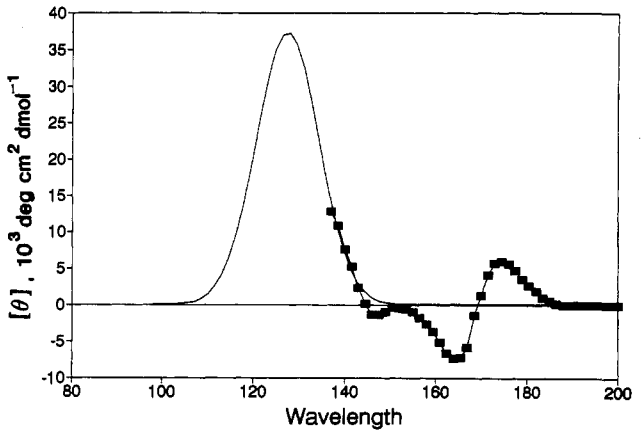

Figure 8. A Gaussian fit to the 135–142-nm VUCD of methyl α-D-mannopyranoside. See text for details.

a Kramers–Kroning transform of the integrated CD band. The weak coupling between the exponential and linear parameters allowed a simple, iterative convergence. For this purpose, the CD at 173 nm in the film spectrum was scaled to the CD intensity at that wavelength observed in solution.[7a] For the Lorentzian band shape λ° = 125 nm ($\Delta\lambda$ = 2.41 nm, $[\theta^\circ] = 1.7 \times 10^5$ deg cm^2 dmol^{-1}). For the Gaussian band shape λ° = 101 nm ($\Delta\lambda$ = 27.4 nm, $[\theta^\circ] = 3.2 \times 10^4$ deg cm^2 dmol^{-1}). The unrealistic bandwidth for the Gaussian band shape suggests that this band is more Lorentzian in character.

A similar treatment of the rising portion of the high-energy CD in the spectrum of methyl α-D-mannopyranoside results in λ° = 133 nm ($\Delta\lambda$ = 1.4 nm, $[\theta^\circ] = 2.0 \times 10^5$ deg cm^2 dmol^{-1}) for the Lorentzian and λ° = 127 nm ($\Delta\lambda$ = 9.7 nm, $[\theta^\circ] = 3.7 \times 10^4$ deg cm^2 dmol^{-1}) for the Gaussian (Figure 8). We conclude that a reasonable estimate for the band center of the first strong σ–σ^* CD band is approximately 120–130 nm.

The μ–μ CD mechanism[18] for σ–σ^* transitions in saccharides has been examined in depth.[9,10] When the set of C–C, C–O, and C–H bond localized transitions are coupled via perturbation theory, the lowest energy CD component regularly agrees in sign with the observed Na_D rotations; a single scaling factor brings magnitudes into almost quantitative agreement.[9b]

A significant feature of the model is the partial localization of the lowest energy component on the acetal group; i.e., for the strongly allowed σ–σ^* transitions, the two ether groups act as a single chromophore. Although the model contains no explicit consideration of symmetry, this result allows an interpretation of the σ–σ^* CD in terms of the strong coupling of two ether chromophores with local C_{2v} symmetry. Thus, the pair of degenerate $A_1 \rightarrow B_2$ (σ–σ^*) transitions, y polarized in each of the local C_{2v} frames (Table II), interact to produce a pair of CD components. The low-energy component has a rotational strength proportional to $\mathbf{R}_{12} \cdot (\mu_1 \times \mu_2)$.[18] In α-pyranosides the acetal geometry is such as to produce a positive band and positive rotation, as observed. For the acetal geometry in β-pyranosides the expression generates negative rotation. This picture provides the

simplest rationalization of the observed anomeric dependence of pyranoside Na_D rotation, which is perhaps the most characteristic feature of the chiroptical properties of saccharides.[20]

The present work indicates that the calculational model overestimates the σ–σ^* splitting of the primary transition located at approximately 90 nm. The 120–130-nm band center of the low-energy component found here is well below the approximately 160 nm value of the model.[9] Methyl α-D-galactopyranoside displays no increasing CD at 140 nm, in spite of its large Na_D rotation, but it is the only exception noted. The model is apparently flawed in its parametrization of transition dipoles and evaluation of the coupling energy; the need for a scaling factor perhaps partially reflects this inadequacy. The present results give guidance for further model refinement.

Acknowledgment. This work was supported by NIH Grant No. GM46465. The authors thank Dr. Slavomir Bystricky for the xylobioside sample.

(20) Hudson, C. S. *J. Am. Chem. Soc.* **1925**, *47*, 268–280.